Modeling and Rendering of Metallic Patinas

Category: Research

Abstract

An important component that has been missing from image synthesis is the effect of weathering. In this paper, we present an approach for the modeling and rendering of one type of weathering—metallic *patinas*. A patina is a film or incrustation on a surface that is produced by the removal of material, the addition of material, or the chemical alteration of a surface. Oxidation, sulphidization, and painting are examples of phenomena that produce patinas.

We represent a surface as a collection of layers. Patinas are simulated with a series of operators, such as "coat," "erode," and "polish," which are applied to the layered structure. The development of patinas is modulated according to an object's geometry and local environmental factors. We introduce a technique to model the reflectance and transmission of light through the layered structure using the Kubelka-Munk model. This representation yields a model that can simulate many aspects of the time-dependent appearance of metals as they are exposed to an atmosphere or treated chemically. We demonstrate the approach with a collection of copper models.

1 Introduction

All materials have an inherent tendency to change in appearance or composition when exposed to the physical and chemical conditions of the surrounding atmosphere. The rate of change is dependent on the material's characteristics and the severity of its exposure to the elements. The deterioration, decay, and change in appearance of materials due to the effects of the surrounding environment are generally termed *weathering*. Specific examples of weathering include the corrosion of metals, efflorescence of stone and brick, fungal attack on organic materials [32], and the wear and tear of everyday life.

Techniques for realistic image synthesis have advanced dramatically in recent years. However, a common criticism of such images is that they look too ideal, that is the objects they depict lack the effects of wear. Since the appearance of all materials changes with exposure to external influences, the ability to accurately model weathering effects is an important domain for synthetic image generation. Previous computer graphics models of materials are based on the physics of idealized surfaces exhibiting ideal diffuse, glossy, or specular reflection. Such idealized materials rarely exist and are hard to produce; for example, BRDF measurement equipment is often calibrated using standard samples (e.g. MgO or Al) that must be carefully protected to prevent contamination. The predicament of contamination is ironic since idealized materials also do not look real. In order to make such idealized computer graphics models of materials look better, animators and modelers often apply multiple textures to modulate surface parameters in an attempt to mimic the natural variation of each parameter. An outstanding example of this approach is the extensive use of texture maps to simulate wear and tear in the recent full length computer generated movie *Toy Story* produced at Pixar [9]. Many texture maps per surface were used to model scuffs, dirt, gouges and so on. The visual effects crew was specifically instructed to do this to create environments that were not perfect and resembled the places the characters were likely to inhabit. Unfortunately, this use of texture maps is labor intensive and somewhat ad hoc. Each texture map must be hand painted and combined using special shaders. It is also very difficult to properly account for certain effects, such as a spill that crosses the boundary between two patches. Our goal is to increase the believability and complexity of weathering effects by building models of real materials that respond to environmental factors and generate a range of appearances.

In addition to its importance in computer graphics, visualization of weathering effects has broad applicability to a variety of additional fields. Moreover, practitioners in other fields have studied weathering effects for many years, and their theories and studies are good sources from which to draw.

- For many applications it is useful to predict how a material will look in the future. For example, in architecture and preservation, it is important to understand how the surfaces of buildings change over time so that buildings may be designed to minimize the consequences of deleterious weathering effects. Since buildings may stand for hundreds of years, much of their final appearance is dominated by weathering effects. Architects would like to predict the future appearance given an initial set of materials and model of the environment. Similar concerns are shared by a number of engineering applications, such as automotive design, civil engineering, and geology [24, 26].

- Conversely, there are applications where modeling weathering interactions is applicable to the inverse problem of understanding the history of an object from its current appearance. The ability to date an object by determining the type of environment it was exposed to, and the duration of the exposure, would be invaluable. Restoration fundamentally involves returning a weathered object to its true initial appearance [7].

- Many materials are created pre-weathered. These materials are treated in various ways to simulate the process of weathering. Since such treatments are highly desirable (from prewashed jeans to fake antiques), it is important to be able to model them [22, 26].

Our long range goal is to develop easily controlled models of weathered materials for computer graphics. This task involves the identification of the basic physical processes underlying their changes and the development of appropriate computer models. Since weathering involves the action of many environmental forces over time, this will require simulating these processes. Such simulations will also give us the ability to visualize changes over time. We expect that different materials may require different modeling effects. For example, stone, wood and metals weather quite differently because their chemistry and material structures are very different. In this paper we consider only the modeling and rendering of metallic patinas as a starting point.

Metals are particularly susceptible to weathering interactions and often develop a characteristic *patina*. The term patination is generally reserved for effects involving the chemical alteration of the surface resulting in a change in color. However, it is used to describe both the results of deliberately applied craft processes and also those resulting from natural corrosion [16, 22]. Metals in general—and the finished metal surface in particular—begin to change under the influence of the atmosphere, or the local chemical environment, as soon as they are exposed. The quality and degree of change is dependent on the particular surrounding conditions, but the resulting surface coloration of copper or bronze, for example, may include ochre, red, brown, and black oxides, with varying degrees of translucency, and a variety of green mineral products. Patination may also involve intense forms of corrosion. Copper and its alloys are particularly interesting, as they have broad aesthetic as well as practical applications. Humans have used copper longer than any other metal, apart from gold, and throughout its history of some 10,000 years it has played an important role in the development of civilization.

1.1 Previous Work

To date, the simulation of weathering effects has been given little explicit attention in the computer graphics literature. Related work exists in three areas: procedural textures and fractal surface growth models, specific weathering models, and models for the reflection from layered surfaces.

Procedural textures [5] can be used to build up complex patterns that often resemble natural effects. The "shade tree" concept of Cook et al. [4] allowed arbitrary procedures to define a different shading model for each surface, as well as lighting and atmospheric optics. Perlin [28] described an entire procedural language to define textures and laid the foundation for the stochastically-generated textures that permeate rendering today. Turk [34] and Witkin and Kass [38] introduced synthetic texture models inspired by biochemical processes. These are effective in creating pigmentation patterns for the coats of fur on animals as well as other effects. Fleischer et al. [6] generate patterns of surface geometric elements, such as scales or thorns, with a biologically motivated cellular development simulation with a constraint to keep the cells on a surface. Fractal surface growth models, used mainly in physics and various branches of engineering, are concerned with the morphology of various pre-formed interfaces and with the dynamics of how the morphology develops over time [1]. For example, some surfaces are formed as a result of a deposition process; others shrink due to etching.

Starting with procedural texture models, several researchers have attempted to simulate weathering effects. Perlin and Hoffert [29] developed a technique by which objects are modeled as distributions of density. One application of this technique is as an erosion model. Becket and Badler [2] modeled surface imperfections through texture specification and generation techniques, which are based on fractal subdivision and simple distribution models. These techniques are useful for simulating the appearance of some surface imperfections. Blinn modeled the appearance of dusty surfaces, given the thickness of the dust layer [3]. However, he did not provide a way to determine automatically the amount of dust that accumulates on a surface. More recently, Hsu and Wong [15] introduced functions for simulating dust accumulation that attempt to mimic the dust adherence process. In addition, Miller [25] proposed a set of algorithms for local and global accessibility shading. The visual effect of shading using these techniques resembles the tarnish on surfaces that have been polished.

A particularly promising approach to modeling the appearance of materials is to treat a surface as a set of layers. For example, a common application of RenderMan is to develop surface descriptions as a series of layers [35]. This allows the placement of a decal on the surface. Another area of interest is the modeling of reflection and transmission of light through layered surfaces. Hanrahan and Krueger [14] present a model for subsurface scattering in layered surfaces in terms of one-dimensional linear transport theory. This model is useful for rendering common layered materials such as skin, snow, and dust. Wolff has also presented a very similar model of subsurface scattering [39]. Finally, Gondek et al. and Westin et al. have recently described systems for computing the BRDF from surfaces with internal structure [10, 37].

Each of the above approaches produces interesting effects, but none provides a physically-based model of weathering interactions.

1.2 Overview

In this paper, we consider the patination of metals as a specific example of weathering effects. We introduce a new representation of textured surfaces for synthetic image generation, which can greatly enhance the realism of renderings of metallic objects with weathered appearances. We begin by briefly reviewing the physical basis of metallic patinas. We then present a representation of a metal surface as a stack of layers and propose a collection of operators that can be applied to the layered structure to produce a taxonomy of patination effects. We also discuss how patinas can be modulated according to environmental factors and the surface geometry. Next, we offer a method of rendering the layered structure. Last, we demonstrate the approach with copper—a metal with broad application and appeal.

2 Physical Basis of Patina Formation

The atmosphere alters the surface of a metal, causing gradual changes that quickly tarnish the metal with a thin, but uneven, dark coloring, and may eventually convert the whole surface into crumbly mineral products. Natural patinas develop primarily as the result of this process of atmospheric corrosion. Similarly, artificial patinas are deliberately induced through various surface treatments designed to mimic and exaggerate the natural processes. In this section, we briefly describe the principal causes of natural and artificial patination.

The corrosion of metals is an electrochemical phenomenon as discovered by Faraday. Through the corrosion process, a relatively complicated system of reacting layers consisting of the metal, corrosion products, surface electrolyte, and atmosphere is formed. The electrochemical process occurs in corrosion cells. The cells can operate only when an electrolyte (water with associated chemicals) is present on the metal surface. The metal diffuses from the base material layer across the mineral layers and reacts with the electrolyte. As the intermediate layers build up they act as a barrier to the diffusion of the metal, and the corrosion process slows down. Thus, a certain amount of corrosion acts to preserve the integrity of the material.

The physical development of patinas has been studied extensively as part of the more general problem of atmospheric corrosion [23, 27]. The exact nature of the surface chemistry underlying the development of surface coatings and the factors that influence how they form and break down are major foci of current corrosion research. Unfortunately, the experimental data to support a physical simulation that would predict the appearance of a metal is not yet available. An exact model would involve explicitly modeling the crystal structure of a metal as well the reaction rates in considerable detail. In our review of the literature, we have not been able to find a single example of work that both simulates patina formation and uses computer graphics to visualize the appearance of the resulting surface. Therefore, in this paper we present a phenomenological model for the development of patinas, based on observed physical behavior. The following discussion is meant to motivate the design of our system.

2.1 Composition and Formation of Copper Patinas

In order to study the development of metallic patinas, we chose copper as a representative metal. Copper patinas are generally regarded as aesthetically pleasing, and much of the use of copper in architecture and sculpture is based on a patina being formed. The formation of the familiar green-blue patina on copper upon exposure to the atmosphere is perhaps the most striking and most common evidence for the interaction of atmospheric trace substances with metal surfaces. Our model, however, is applicable to a wide class of metallic materials including silver, lead, and zinc.

The patinas of copper and copper alloys are classic examples of the layered structures described above. When viewed in cross-section (see Figure 2 [22]) multiple layers are distinctly visible to the eye. Veron and Whitby identified the principal chemical constituents of such natural copper patinas in the 1930s, correcting long-held assumptions regarding their composition [36]. More recently, Franey and Davis [8] and Graedel et al. [12] have carried out a series of investigations, which have provided a detailed picture of the basic composition and formation mechanisms of natural patinas on copper.

Clean copper surfaces exposed to the atmosphere quickly form a thin layer of tarnish that gradually changes with time to a dull brown and then to a reddish brown color, which is indicative of copper oxide, commonly referred to as mineral cuprite [8, 23]. Once this layer is in place, subsequent layers grow much more slowly. The primary chemical constituents of the patina on copper and copper alloys include copper oxides, sulphides, and inorganic and organic copper salts. Copper sulphide is very dark brown, and the sulphide coating forms integrally with the underlying metallic crystal structure. Thus, the sulphide layer often appears relatively shiny. The copper salts, consisting mostly of sulphates, chlorates, and nitrates, come in a wide variety of colors. Copper sulphate causes the characteristic green color of aged copper.

2.1.1 Dependence of Patina on Physical Environment

Figure 1 is a schematic diagram of the patination process as it can be outlined for three environments based on Graedel's observations [11]. This diagram indicates the varying composition of the patina in the environments and average lengths of time for development. The left column is a marine environment characterized by high atmospheric concentrations of chloride, low levels of acidity in associated water droplets or layers, and low levels of reduced and oxidized sulfur gases. This column illustrates the four primary stages of patina growth in marine air. The first and second stages, which are common with the other two environments, involve the formation of a layer of tarnish and a layer of cuprite at the copper surface. The third stage is characterized by the formation of several copper minerals, with atacamite and other chlorine-containing substances expected to predominate because of the high chloride concentration. Small amounts of organic matter are present within the structure and help to bind the individual crystals together. The final stage of the process augments the patina with similar minerals and binding materials.

On land, the controlling processes change and a patina of a different composition is produced. Both rural and urban air have moderate to high concentrations of sulfur. Thus, the transition from the second to the third stage proceeds largely by sulphurization atop the cuprite, with some atacamite being formed as well. The initial form of the sulphur compound is primarily the mineral posnjakite. An organic binder also begins to become incorporated into the patina.

The final stage will differ in the two environments. In the rural case, where acidity and oxidized sulfur concentrations are only moderate, the formation of sulfates will proceed slowly and a mixed patina of atacamite and brochantite is anticipated. In urban areas, a solution with high sulfate concentrations is present, favoring the formation of the basic sulfate minerals antlerite and brochantite, either directly or from pre-existing posnjakite. Organic binding compounds, present in the atmosphere in greater quantities in urban areas, are incorporated into the patina as it forms, where they act to glue newly formed crystals into the patina.

In a marine environment, patinas grow in thickness at an average rate of 1μm per year. In a rural environment, the rate is about $.5\mu$m per year; in an urban environment the rate is $1 - 2\mu$m. These rates are highest during the first few years of exposure and approach a lower, almost negligible rate after about 20 years or so [24].

2.1.2 Developing a Model

Despite the caveats mentioned above, this information permits at least a qualitative prediction of the performance of copper in different environments. In Section 3, we develop a model in which we represent a surface with a collection of layers. Each layer corresponds to a stage in the model described above.

2.1.3 Artificial Patination

It is also common to develop patinas on metals through artificial craft processes. The range of chemical treatments used in artificial patination is very extensive, leading to a wide variety of colors and surface qualities. For example, copper metalwork is routinely immersed in baths of different chemicals, and various washes and rinses are applied. Alternatively chemicals may be dabbed, wiped, or brushed onto the surface. An excellent reference on these processes is the book by Hughes and Rowe [16].

2.2 Environmental Factors

While the preceding section gives a description of the development of patinas in three different environments, including the constituents of the patina and general growth rates, the development can be influenced by a specific surrounding environment. For example, patination in Los Angeles and New York follows the general urban environment model, however, the rate of development is faster in New York due to the greater amount of annual precipitation. The most influential environmental factors in the patination process are the following:

- **Time and Pattern of Wetness.** The time of wetness depends on the relative humidity of the atmosphere, the duration and frequency of precipitation, the temperature of the air and metal surface, the wind speed, and hours of sunshine. The precise shape of the water patterns also significantly affects the appearance of the reaction products. If the position or topography of the surface provides areas in which precipitation is retained as stagnant water, patination occurs more rapidly in these areas. Similarly, horizontal or inclined surfaces patinate more rapidly than vertical surfaces [12], due to their tendency to collect water.

- **Composition of the Surface Electrolyte.** The electrolyte film on the surface contains various substances deposited from the atmosphere or originating from the corroding metal. The electrolyte composition depends on the local atmospheric conditions, and this strongly influences the nature of the chemical buildup on the surface. For example, if a marine environment is adjacent to an industrial site, it may have unusually high concentrations of sulfur, thereby influencing the patination process.

- **Temperature.** The influence of temperature on atmospheric corrosion is complex and has been the subject of many systematic investigations [23, 24]. In general, an increase in temperature stimulates the corrosion attack by enhancing the rate of electro-

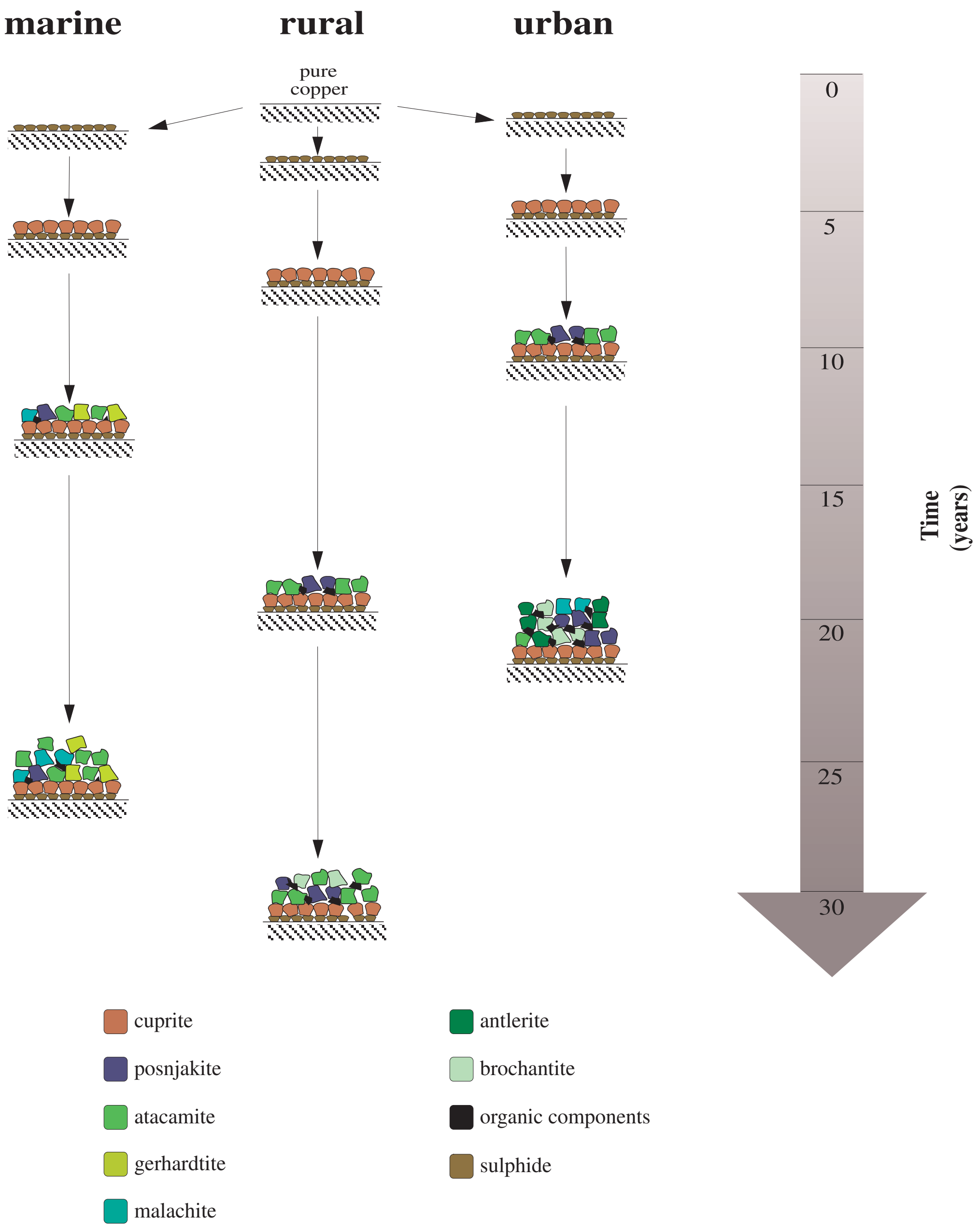

Figure 1: A schematic diagram of the processes involved in the growth of copper patinas in marine, rural, and urban atmospheres.

chemical and chemical reactions as well as diffusion processes. However, an increase in temperature leads to more rapid evaporation of surface moisture; consequently, heat shortens the time of wetness and decreases the amount of corrosion.

Another major factor affecting the appearance of metals is the variation in surface thickness due to abrasions, polishing, and pitting.

In this work, we vary the development of the patina by the time and pattern of wetness as described in Sections 3.2 and 5. Other factors such as temperature could easily be added, as their impact becomes better understood.

3 Modeling

As we observed in the previous section, the development of a metallic patina is a process that proceeds in a complex system of layers. In this section we describe a representation of the structure of a layered material and a set of operators that can be applied to this representation to simulate a variety of effects. By writing a script in terms of these operators, the weathering of the material as a function of time may be simulated.

3.1 Layers and Materials

In our representation, a surface contains a stack of n layers (see Figure 2). The "0"-th layer is assumed to be the base material and is assumed to have essentially infinite thickness. The total thickness of the stack of layers is assumed to be small relative to the area covered by the layer. Each individual layer also has a thickness; if a layer has zero thickness at that point, then that layer is not present at a point. We have varied only the thickness as a function of position, but other properties could be similarly controlled.

The remainder of the material properties do not depend on position. Each layer consists of a homogeneous material. The surface of each material has the standard set of surface shading parameters such as diffuse and specular colors and an overall roughness or shininess. In addition each material has two volumetric properties that control how light is transmitted and reflected due to subsurface scattering in the layer. The light reflection and transmission properties of layers and the rendering of the layer structure are discussed in Section 4.

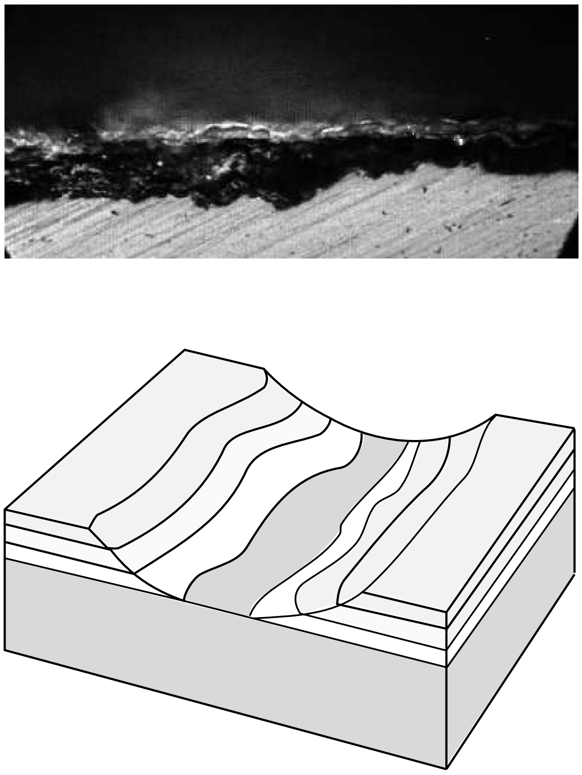

Figure 2: A surface patina as a stack of layers. On the top is a photograph of the cross-section of a copper surface showing the layers. On the bottom is our abstraction of the layered structure.

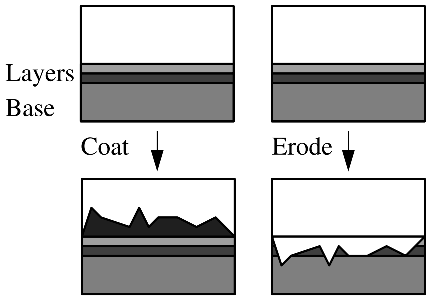

Figure 3: The coat and erode operators.

3.2 Operators

The development of a patina is implemented as a series of operators on layers. By controlling the sequencing of these operators, a wide variety of effects may be created. Our current implementation includes the following operators:

- **coat** *material thickness thickness-map*

  The coat operator adds a new layer of material to a surface. The new layer has a specified maximum thickness which is modulated by the thickness map (see Figure 3).

- **erode** *thickness thickness-map*

  The erode operator removes material from a layered surface. The depth of the erosion may be controlled by a thickness map. The erosion operator proceeds through the stack of layers decreasing the thickness of each layer until the desired amount of material has been removed. If the magnitude of the erosion is small, only the topmost layer will be affected. If, however, the erosion depth is large, multiple layers may be cut through; this provides a means to cut into a material and expose underlying layers. In principle, the amount of an erosion may depend on the hardness of the material in each layer, although our current system does not store hardness as a material attribute (see Figure 3).

- **fill** *material height height-map*

  The fill deposits material up to a given absolute height above the base material. This is somewhat akin to filling all the valleys with water until it reaches a given height. This is a simple way to simulate the deposition material in cracks and crevices.

- **polish** *height height-map*

  The polish operator removes material until a given absolute height above the base material is reached. The result is a smoothing effect across a surface. A variation of the operator removes material until a given area of surface is exposed. This version of the operator was motivated by observing profiles and statistics of rough surfaces after they have been polished [33].

- **offset** *radius*

  The offset operator applies a material to a surface by first applying a thick coat and then removing the part accessible to a sphere of a given radius. The offset surface is computed using techniques described by Miller [25]. (We have implemented both versions of his operator: one computes the largest tangent sphere, the other forms a positive and then a negative offset surface and compares that to the height of the original surface). Note that in Miller's system the offset height is just a parameter used to mix two colors; in our system the offset height is used to control the amount of material added to the layer.

We have implemented a simple scripting language to describe the sequential application of different operators. This can be used simply to assemble a layered surface from a set of materials and texture maps. In this case each material and thickness map represents the current characteristics of the layered surface. This makes it possible to give the user control over the ordering of various operators and special effects such as polishing. Alternatively, the operators can be repeatedly applied to simulate the action of the environment on the surface. When used in this way the scripts may be generated by a program that attempts to cycle through various operations occurring through time. In Section 5 we will show several example scripts.

3.3 Texture/Thickness Maps

The operators we have described are able to model a multi-layered patina, but one that is completely uniform and devoid of the variations and richness of detail that any natural process generates. Next, we will explain a few simple, physically plausible methods to modulate these operators across the surface, simulating the detail present in the real aging process. In our system we have used two representations for spatially-varying thickness maps:

1. **Rectangular texture maps.** In this implementation the thickness is controlled by a standard 2D texture map.

2. **Triangulations as texture maps.** This implementation represents thicknesses as values attached to the vertices of a triangulation.

In order to simulate variations in thickness over time, we have implemented a series of fractal surface growth models for use with the layer structure. Many of these approaches are variations of models from the book by Barabási and Stanley [1]. We chose a set of models that deal with the deposition of material and the lateral growth of patches on surfaces. These models are particularly appropriate for modeling the types of patterns that emerge in the corrosion process, as corrosion typically begins with the deposition of water and particulate matter from the atmosphere onto a surface. Patches develop and spread based on the amount of water and other substances on the surface. Our implementation of these models includes several growth rates, such as linear, parabolic, and logarithmic. We provide the following models:

- **Steady thickening (ST).** This model creates a very simple sequence of maps in which thickness increases with time according to a given growth function. For small time periods it yields a low density pattern with small thickness and for large time periods, it yields a high density pattern with large thickness. The rate of change depends on the growth function. A small amount of noise is added to the pattern to keep the appearance natural.

- **Random deposition (RD).** Random deposition is the simplest growth model. From a randomly chosen site over the surface, a particle falls toward the center of the object until it reaches the top of the surface under it, whereupon it is deposited. We implement this model by randomly chosing a position i and increasing its height $h(i,t)$ by one, where t denotes the time step. A modification of this model, random deposition with surface relaxation, allows the deposited particle to diffuse along the surface up to a finite distance, stopping when it finds the position with the lowest height. As a result of the relaxation process, the final interface—or surface of the layer—will be smooth, compared to the model without relaxation, which is extremely rough.

- **Ballistic deposition (BD).** In the Ballistic deposition model, a particle is also released from a randomly chosen position above a surface. The particle follows a straight vertical trajectory until it reaches the surface, whereupon it sticks. The height of the interface at that point i is increased to max$[h(neighboring_points, t), h(i,t) + 1]$. We also include a variation of the model with a nearest-neighbor sticking rule. In this version, we choose a random position above the surface and allow a particle to fall vertically toward it. The particle sticks to the first site along it trajectory that has an occupied nearest neighbor. Growth is defined quantitatively through simple functions that calculate the mean height of the surface. The key difference between the RD and BD models is that the RD interface is uncorrelated—i.e. the columns at each point on the surface grow independently, since there is no mechanism that can generate correlations along the interface. In BD, the fact that particles are capable of sticking to the edge of neighboring points leads to lateral growth.

- **Directed percolation depinning (DPD).** Starting with a collection of initial patches on a surface, we develop an interface that grows in all directions in two-dimensions. We begin with a simple 2D lattice and mark certain cells as *blocked* and others as *unblocked* and use cellular automata rules to determine which cells get filled in on each cycle. An unblocked cell is much more likely to be filled in than a blocked cell (the rules for it are much less stringent). This process creates bottom level; the upper levels (accounting for variations in thickness) are filled in as follows: the probability of a cell appearing in level $l + 1$ is proportional the number of cells in level l that support it.

  Blocked cells will try to stop the growth, while the interface is free to advance on unblocked cells. In our version of the model, unblocked cells imply concentrations of moisture on the surface and thus stimulate growth.

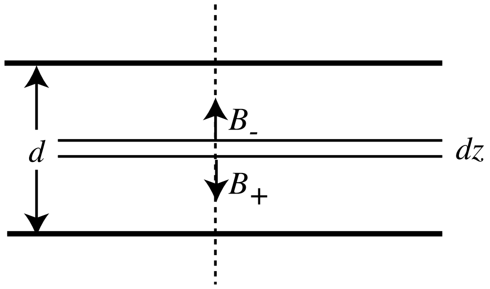

Figure 4: Positive and negative flux density within a layer.

Note that in our current system the development of the layer structure through time is controlled in two ways. In addition to scripting different operations, specific growth models, as described above, can be used to generate thickness maps through time. These growth models can be controlled by environmental factors and the geometry of the surface. Finally, the layer structure is output as a series of material properties and texture maps and passed to the rendering system. This allows additional control over the final appearance of the surface.

The use of development models represents something of a black box in that it is possible to use other procedural models or scanned patterns to generate the thickness maps. In addition to the approaches described above, we also make use of standard procedural texturing approaches, such as noise and turbulence functions [5]. We have found the above models to be especially useful. However, as additional information is learned about the development of patinas, more exact models could be used, without affecting the overall patina modeling framework.

4 Rendering

The appearance of a layered structure is a result of light interacting with the surface and subsurface. Surfaces arise at the interfaces between layers. Light is reflected from the surface depending on the surface roughness and the specular color. The surface reflection gives the layer a glossy appearance. Light is also reflected from and transmitted through the interior depending on the absorption and scattering properties of the material. The subsurface reflection gives the layer a matte or diffuse appearance. The fact that light is also transmitted through the stack of layers causes the colors of different layers to be mixed; it also allows underlying materials to remain partially visible.

4.1 Single Layer

To model reflection and transmission through a single layer we use the Kubelka-Munk (KM) model [21]. The KM model is widely used in the paint, printing, and textile industries to compute diffuse colors due to subsurface scattering [17]. The book by Kortum is an excellent source of information about the KM model [18].

The KM model was recently introduced to computer graphics by Haase and Meyer [13]. In that work the color of a thick layer of paint consisting of several pigments was quantitatively modeled. Given the relative concentrations of several pigments, they were able to predict the final appearance of the paint. The KM model was compared to the standard additive or subtractive color models used in computer graphics and was found to be more accurate. They also used the KM model to estimate the pigment concentrations needed to match a given color. In this work we use the KM model to predict the color effects due to variations in layer thickness, and to predict the color of a stack of layers of different pigments.

The KM model corresponds roughly to 1-dimensional volume radiosity. Figure 4 shows the transport of light within a layer. The KM model assumes that the light distribution is directionally isotropic, but varies as a function of depth. The light distribution therefore is described by the flux density (energy per unit area), or volume radiosity, in the inward or positive, and outward or negative directions, denoted by B_+ and B_-.

As light propagates through the volume it may be absorbed or scattered, according to the following coupled differential equations

$$\begin{aligned} \frac{\partial B_+}{\partial z} &= -(K+S)B_+ + SB_- \\ \frac{\partial B_-}{\partial z} &= SB_+ - (K+S)B_- \end{aligned}$$

where K is the absorption per unit length, and S is the backscattering per unit length. Backscattering decreases the energy flow in one direction, thereby causing an increase in the opposite direction.

These equations have an analytical solution for a homogeneous layer of thickness d [19]. Given these solutions it is possible to compute the reflectance R and transmittance T through a layer:

$$\begin{aligned} R &= \frac{B_-(0)}{B_+(0)} = \frac{\sinh bSd}{a\sinh bSd + b\cosh bSd} \\ T &= \frac{B_+(d)}{B_+(0)} = \frac{b}{a\sinh bSd + b\cosh bSd} \end{aligned}$$

Here $a = (S+K)/S$ and $b = \sqrt{a^2-1}$. Note that in general K and S are functions of wavelength, and hence the calculations involved in the KM model must be performed separately for each color sample.

The major problem in using the KM theory is the determination of the layer parameters K and S. One method is based on the formula for the reflectance of an infinitely thick layer:

$$R_\infty = 1 + \frac{K}{S} + \sqrt{\frac{K}{S}^2 + 2\frac{K}{S}}.$$

This formula can be inverted and the ratio K/S computed from R_∞. Thus, measuring the reflectance of an optically thick sample allows one to compute K/S. Another common

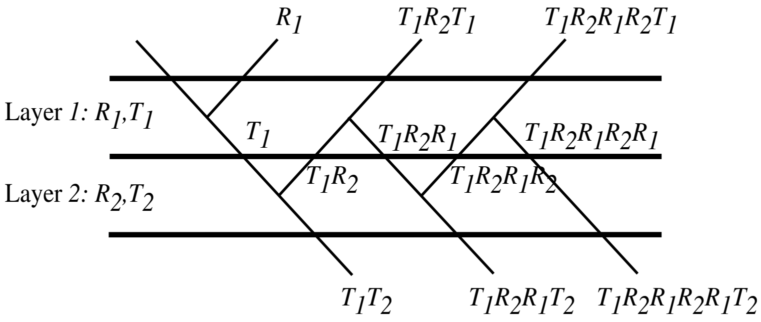

Figure 5: Multiple reflections from two layers.

method for determining the KM parameters is to measure the reflectance of a thick layer and then the reflectance of a layer of known thickness over a background material of known reflectance. A good discussion of different methods for determining the KM parameters in the context of computer graphics is contained in Haase and Meyer[13].

In our work we have estimated the KM parameters by matching synthesized color samples to physical copper and mineral specimens, as well as photographs, such as those found in Hughes and Rowe [16]. We generally match R_∞ to the sample, and then determine K/S from the above formula, and assume a value for S. This approach has enough accuracy to capture the range of colors and color effects that we are attempting to model. A more careful study involving detailed comparisons with physical samples under controlled weathering conditions would require more accurate radiometric and colorimetric measurements. However, this is beyond the scope of this study.

4.2 Multiple Layers

Kubelka also extended his model to account for the reflectance and transmittance due to a stack of layers [20]. If the layer is homogeneous then the transmittance and reflectance are symmetric; that is, they do not depend on whether light is propagating upward or downward. This observation, along with the fact that it is easy to enumerate all possible light paths giving rise to reflection or transmission through two layers, leads to an expression for the reflection and transmission through the two layers that accounts for multiple scattering:

$$\begin{aligned} R &= R_1 + T_1^2 R_2 + T_1^2 R_2 R_1 R_2 + T_1^2 R_2 (R_1 R_2)^2 + \ldots \\ &= R_1 + \frac{T_1^2 R_2}{1 - R_1 R_2} \end{aligned}$$

$$\begin{aligned} T &= T_1 T_2 + T_1 T_2 R_1 R_2 + T_1 T_2 (R_1 R_2)^2 + \ldots \\ &= \frac{T_1 T_2}{1 - R_1 R_2} \end{aligned}$$

This compositing process can be repeated, sequentially combining two layers into a single layer, to account for the reflection and transmission through a stack of n layers. We normally do this front to back, although it can be done in any order. Thus it is essentially no more difficult to compute the diffuse reflectance and transmittance, including all possible transport paths, for a stack of n layers than for a single layer. These formulas may also be used to combine a stack of layers with an opaque base layer. (Note that most formulations of the KM model explicitly include composition with a background layer R_g.)

We call this process *subsurface compositing* to differentiate it from the normal compositing operators widely used in computer graphics [30]. Subsurface compositing differs from normal compositing in that visible light is always assumed to be transmitted through each layer twice, which gives rise to a T^2 factor in front of each reflectance. This lowers the visibility of underlying layers. Subsurface compositing also accounts for the effect of multiple scattering which leads to a $1/(1 - R_1 R_2)$ factor which increases the contribution from each layer. These are important effects when viewing a stack of adjoining layers; it differs from the typical case in computer graphics where a set of disjoint partially transparent reflecting surfaces are being viewed. In this case it is incorrect to only consider one dimensional interreflection, and the light source is not necessarily emanating from the eye.

4.3 BRDF

The above techniques are used during rendering to compute an approximation to the BRDF of each point on the layered surface. We assume the final BRDF consists of a diffuse term and a mixture of glossy terms. The diffuse reflectance of a stack of layers is computed exactly as described above, and needs no further explanation.

Accounting correctly for glossy reflection is more complicated, so we make several assumptions to simplify rendering. Glossiness is caused by light reflection at the interface between layers. Traditionally in computer graphics there is only a single interface between air and the material—the surface itself—and this interface causes the glossy appearance; in a layered structure there are multiple interfaces. In our system we perform the following two steps. First, glossy reflection at each interface is modeled using the standard computer graphics model for shiny surfaces; that is, with a specular color and a Phong microfacet distribution function parameterized by the surface roughness, $C_s(N \cdot H)^{1/r}$. Each interface inherits properties from the material below it, hence, each interface may have a different roughness and color. Second, to account for attenuation due to absorption and scattering in the layers above the interface, the specular color is multiplied twice by diffuse transmittance of the intervening layers calculated using the KM equations. The output glossy BRDF consists of a set of surface roughnesses and attenuated specular colors. The renderer needs to be modified to sum over this set of microfacet distributions when computing the final glossy reflection component. If the final specular color of one of the glossy terms is 0, that usually implies that it has been covered by an opaque material.

This method of computing glossy reflection is an approximation for several reasons. First, it is strictly not correct to use the diffuse transmittance to attenuate the incoming and outgoing radiance because even with a homogeneous layer the transmittance will be a function of direction. Second, the above model does not account for scattering events in the intervening layers before or after the glossy reflection. In general accounting for this would require the full solution of the one-dimensional transport equation, as was done in Hanrahan and Krueger [14]. The precise nature of the errors introduced by these approximations needs further study. But our approximations capture quite well all the major visual effects that we hoped to achieve.

Finally, we output the final thickness of the stack of layers by summing the thicknesses of each layer. This final thickness may be used to either perturb the normals or displace the surface during final rendering.

5 Results

To demonstrate the modeling and rendering approaches described in the paper, we show results from several complex simulations.

5.1 Copper Strips

Plate 1 depicts the weathering of copper strips exposed to marine, rural, and urban environments respectively over the course of a thirty year period (in six year increments). This example shows the possibilities for the development of natural patinas in distinct environments. In all cases, the basic development of the patina was derived from the model presented in Section 2.1. The patterns used in the layer maps were created though the fractal surface growth models described in Section 3.3. The development of the patina was simulated using the layer structure with various combinations of operators. The leftmost strips represent the appearance of pure copper—the starting point for the simulations.

- **Marine environment.** The top row is a simulation of changes due to a typical marine environment. Here, we used the BD and DPD models to vary the thickness of the layers as a function of time. The BD model yields spotty patterns that are characteristic of marine environments, which often leave uneven coatings of moisture and salts on surfaces. The DPD model provides a patchy but more uniform coating of patina in the latter stages. The coatings in the early stages are mainly sulphides and oxides, with very small concentrations of chlorides. The last two stages demonstrate major transformations to the surface. The dark green, orange, and blue combinations are due to large concentrations of sulphates, chlorates, and nitrates. In the last stage, we erode a small portion of the top layer away. The script for the last strip in the series is the following:

  ```
  new copper;
  coat tarnish 0.35 texture(bd110.tif);
  coat cuprite 1.2 texture(dpd2001.tif);
  coat marine_patina1 3.0 texture(bd007.tif)
  coat marine_patina2 1.8 texture(dpd2015.tif);
  ```

```
erode 0.5 texture(bd005.tif);
render maps;
```

- **Rural environment.** The middle row is a simulation of effects common to a typical rural environment. Note that it takes about eighteen years for the green patina to begin to appear here, due to the small amounts of pollution in the surrounding atmosphere. Patinas in rural environments tend to be fairly spatially homogeneous. To capture this quality, we used the ST pattern generator to vary the thickness of the layers in the sequence. The script for the last strip in this series is as follows:

```
new copper;
coat tarnish 0.25 texture(st0.tif);
coat cuprite 1.0 texture(st0.tif);
coat rural_patina1 1.0 texture(st003.tif);
coat rural_patina2 1.1 texture(st008.tif);
render maps;
```

- **Urban environment.** The bottom row is representative of changes due to an urban environment. Here, the films are very thick, reflecting the greater amount of pollution and humidity in the surrounding atmosphere. Note that in this case, the green copper salts begin to appear much earlier in the sequence. About eighteen years into the sequence, the surface is covered with a thick, almost continuous coating that is primarily composed of copper sulphates and chlorides. In this sequence, we used the DPD model to generate the variations in thickness. This model gives rise to fairly continuous patches that grow laterally on the surface. It is common for urban patinas to be very soluble and to develop coatings of soot/dirt. To capture this, we erode away some of the patina and add a layer of dirt on the surface using the RD model on the last strip in the sequence. This is the script for the last strip:

```
new copper;
coat tarnish 0.55 texture(dpd0.tif);
coat cuprite_urban 1.0 texture(dpd2001.tif);
coat patina_urban1 4.0 texture(dpd2002.tif);
coat patina_urban2 3.0 texture(dpd2005.tif);
erode 0.8 texture(dpd020.tif);
coat dirt 1.9 texture(bd002.tif);
render maps;
```

Plate 2 illustrates the layers and the final BRDF parameters for the urban series. Note that the layer structure records the evolution of the strip from bottom to top. It is interesting to observe that each layer has constant surface properties; all the variations in color and texture arise from varying the thickness of the different layers.

Plate 3 shows a sequence of copper strips that display effects that are normally created with artificial patination techniques [16]. Unlike the previous examples, the series is not cumulative. In each case, the effects were simulated by using experimental data to determine the nature of the changes to the surfaces, including colors and film thicknesses. We describe the series from left to right. Strip 1 is a piece of pure copper, indicative of the initial appearance. In strips 2–4, we used patterns scanned from a book on artificial patination as input to the various operators [16]. In strips 5 and 6, the layer maps were generated procedurally. In strip 5, we used a basic noise function [28] and in strip 6, we used the DPD model. Both of these strips have interesting variegated appearances.

5.2 Buddha

Plate 4 shows the development of the patina on a small statue of a buddha. The buddha model was created from a Cyberware scan and consists of approximately 60,000 small evenly sized triangles. In these pictures the table and wall are rendered using conventional texturing techniques, and the buddha is rendered using the techniques described in this paper.

In this experiment the various stages of the development of the patina are simulated in the RenderMan shading language. A shader was written that modeled a three layered surface: base copper, a tarnished layer, and a green patina. Parameters related to thickness are shown as a function of time in Figure 6. The thickness of different layers also depends on position and other factors as follows:

- The thickness of the tarnish layer was computed using two functions. The first, labeled tarnish in Figure 6, models tarnishing due to atmospheric processes. This parameter does not vary spatially. The second parameter, labeled polish, shows the decrease in tarnish thickness due to polishing the buddha. This parameter does vary spatially as determined by the accessibility map (the accessibility map is computed as a preprocess, and therefore there is a single accessibility value per triangle) [25]. Thus, tarnish appears in cracks and crevices, and shiny copper appears in exposed areas.

- The green patina consists of a steadily thickening layer and a set of steadily growing random patches. The steadily thickening layer depends on the local wetness of the surface; the wetter the surface the thicker the patina. The wetness is controlled by a precomputed exposure map that gives the average irradiance due to the sun and sky received by that part of the surface, and a simple function that decreases the average wetness of inclined surfaces. Another simple procedure increases the wetness along the base of the statue where water is likely to accumulate; this effect changes through time under control of the base parameter. The patches of the patina are controlled by a random fractal surface growth process. To show the flexibility of the system, the surface growth pattern is computed using the standard noise function in the shading language. The thickness of these various components of the patina change through time as shown in Figure 6. The curve labeled body controls the thickness of the steadily thickening layer, the curve labeled base controls the thickness along the bottom, and the curve labeled bump controls the thickness of the random growth process.

The left hand column of images shows the development of the tarnish and green patina. The accompanying videotape animates the effect of weathering over time.

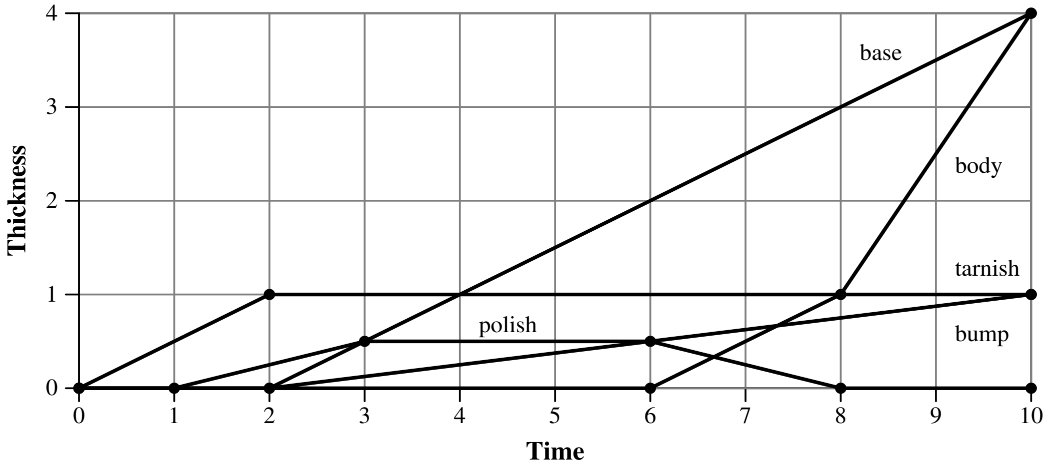

Figure 6: Development of patina on buddha statue.

5.3 Towers

Plate 5 shows two copper-covered towers of different ages in an urban environment. The tower on the left displays a dark cuprite coating due to a few years of exposure; the tower to the right has a green patina typical of several decades of exposure.

For this simulation, we modulated the appearance of the patina based on several functions. As in the previous example, the wetness is controlled by a precomputed exposure map that gives the average irradiance due to the sun and sky received by a regions of the surface and a simple function that decreases the average wetness of inclined surfaces. For example, inclined areas that face south have thinner layers of patina, reflecting the fact that they would be dryer. We also used an accessibility map to vary the thickness of the patinas across the surfaces.

The new dome to the left is covered with a thin layer of cuprite. In addition, some simple texture maps were created with a noise function and combined with the layer structure to simulate the staining due to the flow of water over the top of the dome. Modeling such washing and staining effects will require additional study.

In the dome on the right, there is a thin layer of cuprite on the base copper. This is augmented with a fairly uniform layer of patina. We also added a thin layer of dirt, which is common to urban patinas. All layers are varied by simple noise functions.

6 Summary and Discussion

We have presented an approach for the modeling and rendering of one type of weathering—metallic patinas. A surface is represented as a set of layers. This representation resembles the underlying structure of the physical model of a patina. A set of operators was introduced that when combined with a basic understanding of the physics and chemistry can simulate a wide variety of weathering effects. We also presented an approach to modeling the reflection and transmission through the layer structure using the Kubelka-Munk model. The modeling and rendering approach is capable of simulating a variety of metallic patinas.

Although we attempted to model the development of patinas on surfaces based on the available physical evidence, our model is still a phenomenological one. We believe that an exact model is not possible at this time, as the more general problem of the atmospheric corrosion of metals is not yet fully understood. However, the new layered model would appear to have great usefulness in computer graphics due to the ease with which it is possible to give the designer control over a wide variety of processes important in determining the final appearance of an object.

This representation of a material is significant, as it can accommodate the time-varying nature of a surface and its exposure to a complex class of weathering effects. We believe that this general model will be applicable to other materials as well. The problem of creating physically-based models of real materials, which can incorporate variations over time, is an important topic for computer graphics. This is a difficult problem, as the factors that determine the changes in appearance of materials operate simultaneously and are not completely understood. These difficulties notwithstanding, many interesting research directions remain. One area is in the design of models for other materials, such as wood or plastics. Another topic is the development of more complex operators, which can simulate dynamic processes, such as erosion. Last, we would like to add interactive operators to the system. These would be especially useful for creating patterns due to various brushes used in artificial patination techniques.

References

[1] A. L. Barabási and H. E. Stanley. *Fractal Concepts in Surface Growth*. Cambridge University Press, Cambridge, 1995.

[2] Welton Becket and Norman I. Badler. Imperfection for realistic image synthesis. *The Journal of Visualization and Computer Animation*, 1(1):26–32, January 1990.

[3] J. F. Blinn. Light reflection functions for simulation of clouds and dusty surfaces. In *Computer Graphics (SIGGRAPH '82 Proceedings)*, volume 16, pages 21–29, July 1982.

[4] Robert L. Cook. Shade trees. In *Computer Graphics (SIGGRAPH '84 Proceedings)*, volume 18, pages 223–231, July 1984.

[5] David S. Ebert, editor. *Texturing and Modeling*. Academic Press, New York, 1994.

[6] Kurt Fleischer, David Laidlaw, Bena Currin, and Alan Barr. Cellular texture generation. In *Proceedings of SIGGRAPH '95*, Annual Conference Series, pages 239–248, August 1995.

[7] S. J. Fleming. *Dating in Archaeology*. St. Martin's Press, New York, 1977.

[8] J. P. Franey and M. E. Davis. Metallographic studies of the copper patina formed in the atmosphere. *Corrosion Science*, 27(7):659–688, 1987.

[9] Lawrence French. Toy story. *Cinefantastique*, 27(2):36–37, 1995.

[10] Jay S. Gondek, Gary W. Meyer, and Jonathan G. Newman. Wavelength dependent reflectance functions. In *Proceedings of SIGGRAPH '94*, Annual Conference Series, pages 213–220, July 1994.

[11] T. E. Graedel. Copper patinas formed in the atmosphere - a qualitative assessment of mechanisms. *Corrosion Science*, 27(7):721–740, 1987.

[12] T. E. Graedel, K. Nassau, and J. P. Franey. Copper patinas formed in the atmosphere. *Corrosion Science*, 27(7):639–652, 1987.

[13] C. S. Haase and G. W. Meyer. Modeling pigmented materials for realistic image synthesis. *ACM Tran. Graphics*, 11(4):305–335, October 1992.

[14] Pat Hanrahan and Wolfgang Krueger. Reflection from layered surfaces due to subsurface scattering. In *Proceedings of SIGGRAPH '93*, Annual Conference Series, pages 165–174, August 1993.

[15] S. Hsu and T. Wong. Simulating dust accumulation. *IEEE Computer Graphics and Applications*, 15(1):18–22, 1995.

[16] Richard Hughes and Michael Rowe. *The Colouring, Bronzing and Patination of Metals*. Watson-Guptill Publications, New York, 1991.

[17] Deane B. Judd and Guenter Wyszecki. *Color in Business, Science, and Industry*. John Wiley & Sons, New York, 1975.

[18] G. Kortum. *Reflectance Spectroscopy*. Springer-Verlag, New York, 1969.

[19] P. Kubelka. New contributions to the optics of intensely light-scattering material, part I. *J. Opt. Soc. Am.*, 38:448, 1948.

[20] P. Kubelka. New contributions to the optics of intensely light-scattering material, part II: Non-homogeneous layers. *J. Opt. Soc. Am.*, 44:330, 1954.

[21] P. Kubelka and F. Munk. Ein beitrag zur optik der farbanstriche. *Z. tech. Physik.*, 12:593, 1931.

[22] Susan LaNiece and Paul Craddock. *Metal Plating and Patination*. Butterworth-Heinemann Ltd, Boston, 1993.

[23] Henry Leidheiser. *The Corrosion of Copper, Tin, and their Alloys*. Wiley, New York, 1971.

[24] Einar Mattsson. *Basic Corrosion Technology for Scientists and Engineers*. Ellis Horwood Limited, New York, 1989.

[25] Gavin Miller. Efficient algorithms for local and global accessibility shading. In *Proceedings of SIGGRAPH '94*, Annual Conference Series, pages 319–326, July 1994.

[26] Mohsen Mostafavi and David Leatherbarrow. *On Weathering: The Life of Buildings in Time*. MIT Press, Cambridge, MA, 1993.

[27] R. C. Newman and K. Sieradzki. Metallic corrosion. *Science*, 263:1708–1709, 1994.

[28] Ken Perlin. An image synthesizer. In *Computer Graphics (SIGGRAPH '85 Proceedings)*, volume 19, pages 287–296, July 1985.

[29] Ken Perlin and Eric M. Hoffert. Hypertexture. In *Computer Graphics (SIGGRAPH '89 Proceedings)*, volume 23, pages 253–262, July 1989.

[30] Thomas Porter and Tom Duff. Compositing digital images. In *Computer Graphics (SIGGRAPH '84 Proceedings)*, volume 18, pages 253–259, July 1984.

[31] M. D. Sanderson and J. C. Scully. The initial stages of oxide film formation on copper and some copper alloys. *Corrosion*, 25(7):291–299, July 1969.

[32] John W. Simpson and Peter J. Horrobin. *The Weathering and Performance of Building Materials*. MTP Publishing Co, London, 1970.

[33] T. R. Thomas, editor. *Rough Surfaces*. Longman, New York, 1982.

[34] Greg Turk. Generating textures for arbitrary surfaces using reaction-diffusion. In *Computer Graphics (SIGGRAPH '91 Proceedings)*, volume 25, pages 289–298, July 1991.

[35] Steve Upstill. *The Renderman Companion*. Addison-Wesley, New York, 1990.

[36] W. H. J. Vernon and L. Whitby. The open air corrosion of copper, a chemical surface patina. *Journal Instit. of Metals*, 42(6):181–195, 1932.

[37] Stephen H. Westin, James R. Arvo, and Kenneth E. Torrance. Predicting reflectance functions from complex surfaces. In *Computer Graphics (SIGGRAPH '92 Proceedings)*, volume 26, pages 255–264, July 1992.

[38] Andrew Witkin and Michael Kass. Reaction-diffusion textures. In *Computer Graphics (SIGGRAPH '91 Proceedings)*, volume 25, pages 299–308, July 1991.

[39] Lawrence B. Wolff. Diffuse reflection from smooth dielectric surfaces. In *SPIE Proceedings*, volume 1995, pages 26–44, 1993.